Dalton Transactions

ROYAL SOCIETY OF CHEMISTRY

COMMUNICATION

View Article Online
View Journal | View Issue

Cite this: *Dalton Trans.*, 2024, **53**, 882

Received 27th November 2023,
Accepted 20th December 2023

DOI: 10.1039/d3dt03976e

rsc.li/dalton

An anionic beryllium hydride dimer with an exceedingly short Be···Be distance†

Terrance J. Hadlington

Heteroleptic hydride complexes of the group 2 metals have seen considerable attention as Earth-abundant synthetic tools, yet anionic derivatives are exceedingly rare. We described the facile synthesis and in-depth characterisation of an anionic beryllium hydride dimer, featuring a dynamic [Be_2H_3] cluster at its core with a short Be···Be distance. Despite this, there is no formal Be–Be bond in this complex, with only hydride bridging interactions leading to this remarkable structural attribute.

Main group metal hydrides are ubiquitous in chemical synthesis and as synthons in catalysis. As such, this broader class of compounds remains a field of intensive study, particularly in regards to uncovering fundamentally unique systems, and hitherto unknown reactivity.[1] The s-block metal hydrides are perhaps historically the most utilised, the neutral binary systems (*e.g.* LiH, KH, CaH_2) being main-stays of the modern laboratory as drying agents and synthetic building-blocks, and even as candidates for hydrogen storage materials.[2] Heteroleptic hydride complexes of the group 2 metals (*i.e.* LMH; M = Be–Ba, L = anionic ligand) have been investigated fervently in recent years, due to their well-defined and potent hydridic chemistry,[1a] such as alkene insertion and arene deprotonation,[3,4] in addition to their capacity in catalytic regimes.[1a,4c,5] Until very recently, however, well-defined hydride complexes of the group 2 elements were limited to cationic and neutral species.[6,7] This may be due to the high relative electropositivity of the group 2 elements, leading to highly polarised, and thus highly reactive M–H fragments. Indeed, a recent report from Hicks and co-workers supports this notion, whereby anionic Mg and Ca hydride complexes **A** and **B** rapidly insert carbon monoxide (Fig. 1).[8] These, alongside the beryllium species [{($Et_2BeH)_2$}Na_2] (*viz.* **C**, Fig. 1),[9] are the only structurally characterised examples of anionic hydride complexes of the group 2 metals. We note that further characterisation data for **C** are lacking. Still, Coates and co-workers pioneered earlier work regarding the formation of anionic beryllium hydride species, and indeed broader beryllium hydride chemistry.[10] Ashby and co-workers also developed synthetic methodologies for simple hydrido-magnesiates, $MMgR_2H$ (M = Na, K; R = ^{s}Bu, ^{n}Bu),[11] which are closely related to **A**, though their chemistry is ill explored. In our own work, we are particularly interested in the chemistry of beryllium hydride species,‡ given that this remains one of the few seldom explored territories in metal-hydride chemistry. Indeed, early work from Coates, though again lacking in contemporary characterisation methods, demonstrated that beryllium hydrides should be highly reactive,[10] despite the highly covalent character of the Be–H bond. Our own work has also shed some light on this point: complex **D**, which features a chelating phosphine-appended amido ligand, generates a dimeric beryllium formyl compound through insertion of carbon monoxide into the Be–H moiety.[12] We now demonstrate that reducing the amide

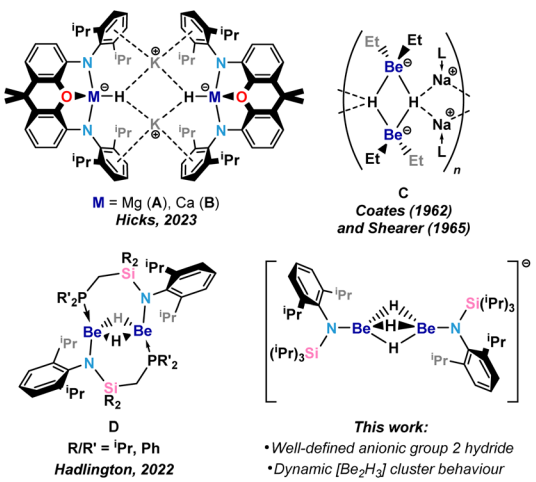

Fig. 1 Known structurally characterised anionic group 2 hydride complexes (**A–C**), our own previously reported heteroleptic beryllium hydride complexes, **D**, and the anionic complex reported here.

Fakultät für Chemie, Technische Universität München, Lichtenbergstraße 4, 85747 Garching, Germany. E-mail: terrance.hadlington@tum.de

†Electronic supplementary information (ESI) available. CCDC 2303227–2303229. For ESI and crystallographic data in CIF or other electronic format see DOI: https://doi.org/10.1039/d3dt03976e

ligand coordination number in employing a monodentate bulky amido ligand allows for the generation of an anionic beryllium polyhydride complex, through formal delivery of $[H]^-$ to a neutral amido beryllium hydride. The triply hydride-bridged anion features a $[Be_2H_3]^+$ cluster core with a Be···Be distance considerably shorter than those calculated and observed in beryllium(I) dimers. Supported by computational insights, it is apparent that this is enforced by the three bridging hydride ligands, forming three 3-centre-2-electron bonds with the Be centres.

In a similar manner to our earlier reported phosphine-chelated amido beryllium halide complexes,[12] complex **1** was accessed through addition of toluene to a rapidly stirred solid mixture of L*K (L* = $[(^iPr_3Si)(Dipp)N]^-$; Dipp = 2,6-$^iPr_2C_6H_3$)[13] and $[Br_2Be{\cdot}(Et_2O)_2]$,[14] precooled to −80 °C. The resulting amido beryllium bromide complex is remarkably soluble, with up to 2 g dissolving in 10 mL heptane at ambient temperature. Storing these saturated solutions at −40 °C leads to crops of crystalline **1**, single crystal X-ray diffraction (XRD) analysis of which revealed a monomeric etherate structure with a three-coordinate Be centre (Fig. S20†). Structural aspects of **1** are in-keeping with previously reported monomeric heteroleptic beryllium halide complexes.[15]

Our goal in employing a bulky, monodentate and monoanionic ligand was to access the likely highly reactive low-coordinate beryllium hydride, [L*BeH] (Scheme 1). Reaction of heptane solutions of bromide complex **1** with $[Li(HB^sBu_3)]$, without stirring, led to the formation of large colourless crystals after room-temperature storage for 24 h. These, however, were not found to be the target neutral beryllium hydride. Rather, the anionic hydride $[L^*Be(\mu\text{-}H)_3BeL^*]^-$ (**2**) was identified by XRD analysis, featuring the $[(THF)_3{\cdot}Li(\mu\text{-}Br)Li{\cdot}(THF)_3]^+$ counterion (**2a**, Scheme 1). This species presumably arises from the initial formation of the desired neutral hydride system, which rapidly reacts with a further equivalent of the hydride source in forming **2a**. This product selectively forms, albeit in poor yields, even when a sub-stoichiometric amount of $[Li(HB^sBu_3)]$ is employed. Though the connectivity in the anionic part of **2a** is clear, significant disorder in the cationic part rendered this data set unpublishable. However, conducting the reaction in the presence of *N*,*N*′,*N*′,*N*′-tetramethylethylenediamine (TMEDA) allows for the isolation of charge separated anion **2** with the $[(TMEDA)_2{\cdot}Li]$ counterion (**2b**, Scheme 1 and Fig. 2). Compounds **2a** and **2b** represent rare examples of structurally characterised beryllates, and indeed the first examples of salt-separated hydrido-beryllates. Both are colourless crystalline solids, which are indefinitely stable under an inert atmosphere, both as solids and in aprotic organic solvents, but are highly moisture and air sensitive. The ^{1}H NMR spectra for both complexes reveal a single Be–*H* resonance at δ = 2.00 ppm in d_8-THF, and δ = 2.64 ppm in C_6D_6. This resonance is broadened, presumably due to the quadrupolar ^{9}Be nucleus, and significantly high-field shifted when compared with our reported neutral beryllium hydrides complexes (*e.g.* **D**: for R = Ph, R′ = ^{i}Pr, δ = 3.81 ppm).[12] This is in line with the hydride ligands being considerably more shielded than known examples, due to the anionic nature of the $[L^*{}_2Be_2H_3]$ moiety in **2**. That one signal is observed for the three hydride ligands in **2** may suggest that a dynamic $[Be_2H_3]$ core on the NMR timescale. Comparing the ^{9}Be NMR spectra of **2b** with our previously reported amido-beryllium hydride complexes **D**, a high-field shift is again observed (*e.g.* **D**: for R = Ph, R′ = ^{i}Pr, δ = 5.1 ppm; **2b**: δ = −4.2), due to the increased charge density at the Be centres in this compound, and is a known effect for electron rich beryllium systems.[16,17] Specifically, this ^{9}Be NMR shift for **2b** is at the lower range for 4-coordainte Be systems, which are typically found from −1.5 ppm to lower field, with a peak width at half height ($\omega_{1/2}$) of 120 Hz, in agreement with heteroleptic beryllium organometallics reported earlier.[14–16] Calculated Be–H IR stretching frequencies (1542 and 1578 cm^{-1}) align with broadened bands observed in the IR spectra of **2a** (1530 cm^{-1}) and **2b** (1540 cm^{-1}).

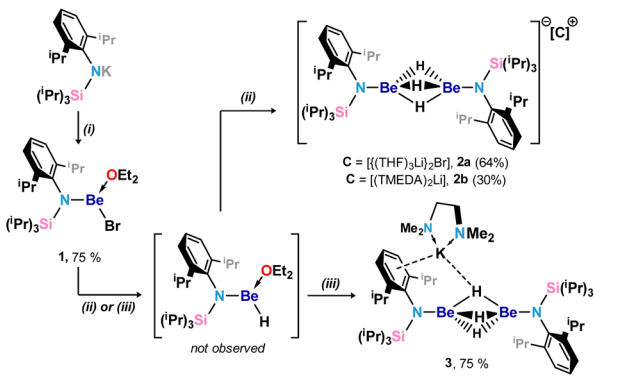

Scheme 1 Synthetic access to compound **1**, **2a/b**, and **3**. (i) $BeBr_2{\cdot}(Et_2O)_2$, toluene, −80 °C–RT; (ii) $[Li(HB^sBu_3)]$ (1 M, THF), heptane, −80 °C–RT, – LiBr (**2a**) or 2LiBr (**2b**, in the presence of TMEDA), – $^sBu_3B$; (iii) $[K(HB^sBu_3)]$ (1 M, THF), heptane/TMEDA, −80 °C–RT, – 2KBr, – $^sBu_3B$.

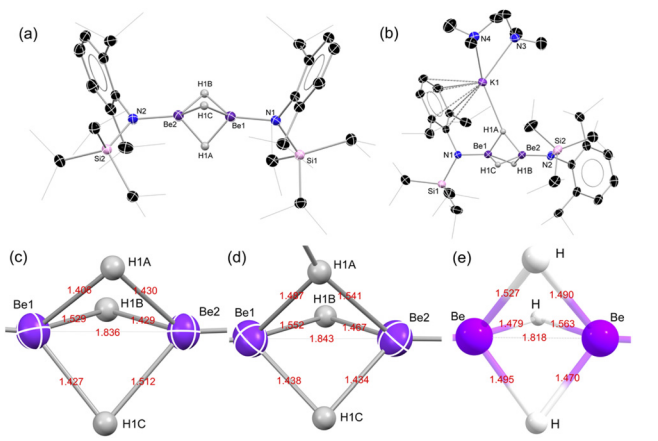

Fig. 2 Above: the molecular structures of (a) the anionic part in **2b**, and (b) the full molecule of **3**, with thermal ellipsoids at 30% probability, and H atoms removed for clarity, aside from [Be–*H*] ligands. Below: a magnified view of the $[Be_2H_3]$ core in (c) **2b**, (d) **3**, and (e) the DFT-optimised structure of **2**.

The solid-state structure of **2b** indicates that no close-contacts are present between the anionic and cationic parts of this compound (Fig. S21 in ESI†). At the core of the anionic part sits a discrete electron-deficient $[Be_2H_3]^+$ cluster, supported at the Be centres by the bulky $[L^*]^-$ ligands. This core is reminiscent of those observed in Me_5PACP-stabilised (Me_5PACP = 1,4,7,10,13-pentamethyl-1,4,7,10,13-pentaazacyclopentadecan) cationic $[M_2H_3]$ hydride species (M = Ca, Sr) recently reported by Okuda and co-workers, despite the differing charge situation.[18] The Be–H distances range from 1.405(3) to 1.529(2) Å, slightly longer than the sum of the covalent radii for these elements (1.27 Å),[19] but in keeping with reported values for bridging Be–H–Be units.[12] More noteworthy is the Be–Be distance: this is remarkably short, at just 1.836(4) Å, significantly shorter than the sum of covalent radii (1.92 Å). Further, this value is shorter than that in the recently reported Be^I dimer, $(CpBe)_2$, which features a Be–Be bond distance of 2.0545(18) Å,[14] and even more so than DFT-investigated $(^R$NacnacBe$)_2$ derivatives (^{R}Nacnac = $[(RNCH)_2CH]^-$), with values of 2.162 Å (R = Me) and 2.134 Å (R = Ph).[20] Still, given the geometry at the Be centres in **2** it is unlikely that a formal Be–Be bonding interaction is present. It is most likely that the highly cationic nature of the Be^{2+} ion, alongside its small size, leads to a close Be···Be distance through the favourable nature of the bridging hydride interactions (*vide infra*).

In an attempt to attain the target neutral beryllium hydride complex, beryllium bromide complex **1** was also reacted with $[K(HB^sBu_3)]$. Here, we believed that the precipitation of KBr may favour the initial salt-metathesis step. This, however, was not the case, with the contact ion pair **3** isolated in good yield (Scheme 1 and Fig. 2(b)). Again, this product is selectively formed even when a sub-stoichiometric amount of $[K(HB^sBu_3)]$ is added, indicating that intermediary [L*BeH] is more reactive than starting material **1**. The [(TMEDA)·K] unit forms an η^6-interaction with one Dipp group of the L* ligand, and a close contact with one hydride bridging ligand. The former arene interaction is reminiscent of those in a number of anionic s- and p-block systems reported recently,[21] and is likely important in the stabilisation of **3**. This only slightly affects bonding in the central $[Be_2H_3]$ unit of **3** relative to that in **2**, with a slight increase in the mean Be–H distance (in **2b**: 1.46(2) Å; in **3**: 1.48(4) Å), and a slight increase in the Be–Be distance to 1.843(8) Å. Some charge distribution from Be to K is further borne out by the slight contraction of the Be–N bonds in **3** (Table 1), indicative of strengthening of this bond compensating for reduced negative charge density at Be. As for **2b**, the hydride signal for **3** presents as a broad singlet in the ^{1}H NMR spectrum (δ = 2.19 ppm), again indicative of fluctional behaviour of the hydride ligands, despite coordination to the $[K(TMEDA)]^+$ counterion.

To gain further insights into the nature of the bonding in the $[Be_2H_3]$ core of these species, we employed DFT and QTAIMs computational methodologies. Primarily, the full molecular structure of the anionic part in **2** was optimised. For comparison, this was conducted with two different functionals, namely B97 and B3LYP, at the def2-TZVP(Be,N,Si)//def2-SVPlevel of theory with D3 dispersion corrections. Solvent effects were considered using the SMD model, for benzene and THF. Optimised structures in absence of calculated solvation lead to shorter Be–H bonds, which, for B3LYP, are on average closest to the experimentally observed values. Calculated Be–N values in this case are also close to the real values, suggesting an accurate picture of the charge distribution in **2**. Still, a contracted Be–Be distance of 1.800 Å is observed here, possibly indicative of an increased charge density in this unit. Solvation, which typically leads to greater and indeed more realistic charge distribution, leads to an increase in Be–H distances in all cases. On the whole, however, B3LYP//def2-TZVP in combination with the SMD-THF solvent model gives the best overall representation of **2**, when compar-

Table 1 Selected bond lengths (Å) for the anionic part in **2b**, **3**, and DFT-optimised **2** [a]

	Experimental		Calculated (B97, *B3LYP*)		
	2b	**3**	Gas-phase	SMD: benzene	SMD: THF
Be1–Be2	1.836(4)	1.843(8)	**1.827**	**1.839**	**1.849**
			1.800	*1.807*	*1.818*
Mean Be–H	1.46(2)	1.48(4)	**1.515**	**1.519**	**1.522**
			1.498	*1.501*	*1.504*
Be1–N1	1.607(3)	1.597(6)	**1.616**	**1.616**	**1.613**
			1.602	*1.599*	*1.603*
Be2–N2	1.607(3)	1.582(7)	**1.618**	**1.618**	**1.617**
			1.605	*1.605*	*1.599*
H1A-K1	—	2.72(4)	—	—	—

[a] The full molecule of **2** was optimised at both B97-D3 and B3LYP-D3 levels, in the gas-phase, and also using the SMD solvent model. The def2-TZVP functional was used for Be, N, and Si. def2-SVP was used for all other atoms.

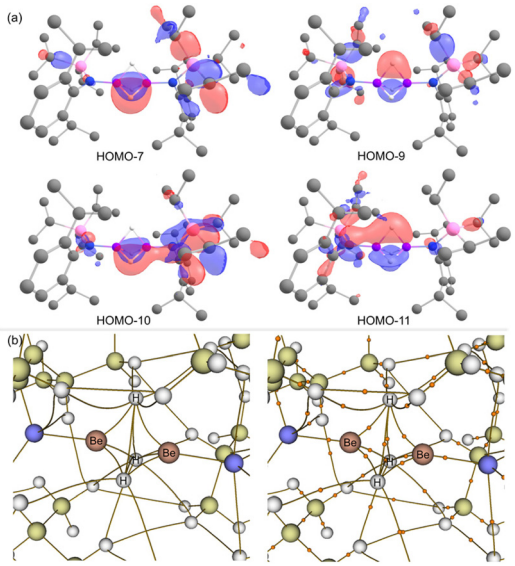

Fig. 3 (a) Selected HOMOs for the optimised structure of **2**, representing the bonding in the $[Be_2H_3]$ core of this compound, and (b) QTAIM-derived bond paths with (right) and without (left) bond critical points.

Table 2 Metrical parameters and FIA values for model neutral hydride complex [(L′BeH)$_2$], and for the anionic congener[a]

	d(Be–Be), Å		Mean d(Be–H), Å		HIA	
	Gas-phase	SMD-THF	Gas-phase	SMD-THF	Gas-phase	SMD-THF
[(L′BeH)$_2$]	1.951	1.972	1.463	1.469	384.9	664.8
[L′Be(μ-H)$_3$BeL′]$^-$	1.806	1.826	1.510	1.515	—	—

[a] HIA values calculated using isodesmic anchoring the $Me_3SiH/[Me_3Si]^+$ reference system (see ref. 17).

ing calculated and experimental data (Table 1). Observing the frontier orbitals of this optimised structure, the HOMO (highest occupied molecular orbital) and HOMO−1 each represent electron density at hydride ligands, and nitrogen lone pairs (Fig. S22 in ESI†), whilst the HOMO−7 and HOMO−9 to HOMO−11 largely represent 3-centre-2-electron bonds of Be–H–Be linkages (Fig. 3(a)), with some delocalisation to nitrogen centres presumably due to N → Be donation. No orbitals were found which represent a direct Be–Be interaction. A topological analysis utilising Bader's QTAIMs further supports these observations (Fig. 3(b)). That is, no bond critical point is observed between the two beryllium centres, but are clearly found between the Be centres and each hydride ligand, further supporting the presence of three 3-centre-2-electron bonds. Paths are also found between each hydride ligand, which also incites formal cluster character in the [Be_2H_3] core. The calculated Mayer bond order (MBO) for the Be–Be interaction is in fact quite large, at 0.53, though this is likely an artefact of the aforementioned cluster character, leading to an 'artificial' bond order. MBOs between 0.28 and 0.65 are found for Be–H interactions (Table S2 in ESI†), also in agreement with a highly delocalised bonding nature.

Finally, to computationally address the formal Lewis acidity of the Be centre in the targeted neutral dimeric hydride complex [(L*BeH)$_2$], the HIA (hydride ion affinity) for the model structure [(L′BeH)$_2$] (L′ = [(Me$_3$Si)(Xyl)N]$^-$; Xyl = 2,6-$Me_2C_6H_3$) was determined using isodesmic anchoring to the $Me_3SiH/[Me_3Si]^+$ couple, in both the gas phase, and using a THF solvent model (Table 2). Employing this solvent model has a large effect on the stabilisation of the anionic **2**, with a highly favourable HIA of 664.8, comparing to 384.9 in the gas phase. The former value is taken as more accurate, given the importance of solvation for charged species. This is a remarkably high HIA value, and in fact may classify neutral [(L*BeH)$_2$] as a Lewis super acid.[22] We are presently developing synthetic methodologies to access this neutral system and related complexes featuring low-coordinate beryllium, to further define such Lewis acidic parameters.

In conclusion, we report a facile synthetic approach to stable, crystalline anionic beryllium hydride dimers featuring [Be_2H_3] cores, best described as discrete beryllium hydride clusters. Computational orbital and topological analyses give key insights into the electron-sharing nature of the Be–H and H–H interactions in this core, displaying three 3-centre-2-electron bonds. These findings give a new perspective on the bonding nature of hydride systems of the lightest member of group 2.

Conflicts of interest

There are no conflicts to declare.

Acknowledgements

T. J. H. thanks the Fonds der Chemischen Industrie (FCI) for generous funding of this research through a Liebig Stipendium, the DFG for an Independent Research grant (project no. HA 9030/5-523956566), and the Technical University Munich for the generous endowment of TUM Junior Fellow Funds.

References

‡We note that one must take precautions when working with beryllium and its compounds, due to health risks associated with this element. See ESI† for further details.

1 (*a*) S. Harder, *Chem. Commun.*, 2012, **48**, 11165–11177; (*b*) M. D. Roy, A. A. Omaña, A. S. S. Wilson, M. S. Hill, S. Aldridge and E. Rivard, *Chem. Rev.*, 2021, **121**, 12784–12965.

2 (*a*) W. Grochala and P. P. Edwards, *Chem. Rev.*, 2004, **104**, 1283; (*b*) N. Klopčič, I. Grimmer, F. Winkler, M. Sartory and A. Trattner, *J. Energy Storage*, 2023, **72**, 108456.

3 For examples of alkene insertion, see: (*a*) J. Spielmann and S. Harder, *Chem. – Eur. J.*, 2007, **13**, 8928–8938; (*b*) M. Rauch, S. Ruccolo and G. Parkin, *J. Am. Chem. Soc.*, 2017, **139**, 13264–13267; (*c*) L. Garcia, C. Dinoi, M. F. Mahon, L. Maron and M. S. Hill, *Chem. Sci.*, 2019, **10**, 8108–8118; (*d*) K. Watanabe, J. H. Pang, R. Takita and S. Chiba, *Chem. Sci.*, 2022, **13**, 27.

4 (*a*) A. S. S. Wilson, M. S. Hill, M. F. Mahon, C. Dinoi and L. Maron, *Science*, 2017, **358**, 1168–1171; (*b*) B. Rösch, T. X. Gentner, H. Elsen, C. A. Fischer, J. Langer, M. Wiesinger and S. Harder, *Angew. Chem., Int. Ed.*, 2019, **58**, 5396–5401; (*c*) S. Brand, H. Elsen, J. Langer, S. Grams and S. Harder, *Angew. Chem., Int. Ed.*, 2019, **58**, 15496–15503.

5 M. S. Hill, D. J. Liptrot and C. Weetman, *Chem. Soc. Rev.*, 2016, **45**, 972–988.
6 For the first examples of neutral heteroleptic group 2 hydrides (for Be–Ba), see: (*a*) R. Han and G. Parkin, *Inorg. Chem.*, 1992, **31**, 983–988; (*b*) D. J. Gallagher, K. W. Henderson, A. R. Kennedy, C. T. O'Hara, R. E. Mulvey and R. B. Rowlings, *Chem. Commun.*, 2002, 376–377; (*c*) S. Harder and J. Brettar, *Angew. Chem., Int. Ed.*, 2006, **45**, 3474–3478; (*d*) C. N. de Bruin-Dickason, T. Sutcliffe, C. A. Lamsfus, G. B. Deacon, L. Maron and C. Jones, *Chem. Commun.*, 2018, **54**, 786–789; (*e*) A. Causero, G. Ballmann, J. Pahl, H. Zijlstra, C. Färber and S. Harder, *Organometallics*, 2016, **35**, 3350.
7 For the first examples of cationic group 2 hydrides (for Mg, Ca, and Sr), see: (*a*) D. Martin, K. Beckerle, S. Schnitzler, T. P. Spaniol, L. Maron and J. Okuda, *Angew. Chem., Int. Ed.*, 2015, **54**, 4115–4118; (*b*) V. Leich, T. P. Spaniol and J. Okuda, *Inorg. Chem.*, 2015, **54**, 4927–4933; (*c*) D. Mukherjee, T. Höllerhage, V. Leich, T. P. Spaniol, U. Englert, L. Maron and J. Okuda, *J. Am. Chem. Soc.*, 2018, **140**, 3403–3411.
8 J. S. McMullen, R. Huo, P. Vasko, A. J. Edwards and J. Hicks, *Angew. Chem., Int. Ed.*, 2023, **62**, e202215218.
9 (*a*) G. E. Coates and G. F. Cox, *Chem. Ind.*, 1962, 229; (*b*) N. A. Bell and G. E. Coates, *J. Chem. Soc.*, 1965, 692; (*c*) G. W. Adamson and H. M. M. Shearer, *Chem. Commun. (London)*, 1965, 240–240.
10 For some examples, see: (*a*) G. E. Coates and G. L. Morgan, Organoberyllium Compounds, in *Advances in Organometallic Chemistry*, ed. F. G. A. Stone and R. West, Academic Press, 1971, vol. 9, pp. 195–257; (*b*) U. Blindheim, G. E. Coates and R. C. Srivastava, *J. Chem. Soc., Dalton Trans.*, 1972, 2302–2305; (*c*) R. A. Andersen and G. E. Coates, *J. Chem. Soc., Dalton Trans.*, 1974, 1171–1180.
11 E. C. Ashby, R. Arnott and S. Srivastava, *Inorg. Chem.*, 1975, **14**, 2422–2426.
12 T. J. Hadlington and T. Szilvási, *Nat. Commun.*, 2022, **13**, 461.
13 (*a*) B. Shen, L. Ying, J. Chen and Y. Luo, *Inorg. Chim. Acta*, 2008, **361**, 1255–1260; (*b*) I. C. Cai, M. I. Lipschutz and T. D. Tilley, *Chem. Commun.*, 2014, **50**, 13062–13065; (*c*) I. C. Cai, M. S. Ziegler, P. C. Bunting, A. Nicolay, D. S. Levine, V. Kalendra, P. W. Smith, K. V. Lakshmi and T. D. Tilley, *Organometallics*, 2019, **38**, 1648–1663.
14 A. Paparo and C. Jones, *Chem. – Asian J.*, 2019, **14**, 486–490.
15 (*a*) C. Helling and C. Jones, *Chem. – Eur. J.*, 2023, **29**, e202302222; (*b*) M. R. Buchner, L. R. Thomas-Hargreaves, C. Berthold, D. F. Bekiş and S. I. Ivlev, *Chem. – Eur. J.*, 2023, **29**, e202302495.
16 J. K. Buchanan and P. G. Plieger, *Z. Naturforsch., B: J. Chem. Sci.*, 2020, **75**, 459–472.
17 J. T. Boronski, A. E. Crumpton, L. L. Wales and S. Aldridge, *Science*, 2023, **380**, 1147–1149.
18 (*a*) V. Leich, T. P. Spaniol, L. Maron and J. Okuda, *Angew. Chem., Int. Ed.*, 2016, **55**, 4794–4797; (*b*) T. Höllerhage, T. P. Spaniol, A. Carpentier, L. Maron and J. Okuda, *Inorg. Chem.*, 2022, **61**, 3309–3316.
19 B. Cordero, V. Gómez, A. E. Platero-Prats, M. Revés, J. Echeverría, E. Cremades, F. Barragan and S. Alvarez, *Dalton Trans.*, 2008, 2832–2838.
20 S. A. Couchman, N. Holzmann, G. Frenking, D. J. D. Wilson and J. L. Dutton, *Dalton Trans.*, 2013, **42**, 11375–11384.
21 For key recent examples, see ref. 8, and: (*a*) J. Hicks, P. Vasko, J. M. Goicoechea and S. Aldridge, *Nature*, 2018, **557**, 92–95; (*b*) R. J. Schwamm, M. D. Anker, M. Lein and M. P. Coles, *Angew. Chem., Int. Ed.*, 2019, **58**, 1489–1493; (*c*) H.-Y. Liu, R. J. Schwamm, S. E. Neale, M. S. Hill, C. L. McMullin and M. F. Mahon, *J. Am. Chem. Soc.*, 2021, **143**(42), 17851–17856.
22 P. Erdmann and L. Greb, *ChemPhysChem*, 2021, **22**, 935–943.